Int J Adv Manuf Technol (2016) 85:825–841
DOI 10.1007/s00170-015-7949-6

ORIGINAL ARTICLE

Performance and wear analysis of polycrystalline diamond (PCD) tools manufactured with different methods in turning titanium alloy Ti-6Al-4V

Guangxian Li[1] · **Mohammad Zulafif Rahim**[1] · **Songlin Ding**[1] · **Shoujin Sun**[1]

Received: 31 May 2015 / Accepted: 4 October 2015 / Published online: 27 October 2015

Abstract Polycrystalline diamond (PCD) tools have been widely used in industry because of its ultra-hardness and high abrasion resistance. Electrical discharge grinding (EDG) and conventional abrasive grinding are currently the two main processes to manufacture PCD tools. However, PCD tools fabricated by the two methods show different cutting performance. This paper investigates the quality and performance of PCD tools manufactured by the two methods in turning titanium alloy. Flank wear, crater wear, tool nose wear, and their mechanisms were investigated; residual stress and graphitization were analyzed quantitatively by using Raman spectrum. Although PCD tools machined with the two methods do not have obvious big difference in visible surface quality, serious tool wear was found on the surface and cutting edge of the conventionally ground PCD tool, while PCD tools machined with EDG process showed better tool wear resistance. Through analysis of Raman spectrum, compressive residual stress of 0.54 GPa was found on the surface of conventionally ground PCD tool. In contrast, larger tensile residual stress was found on the PCD tools manufactured with EDG process.

✉ Guangxian Li
s3463966@student.rmit.edu.au

Mohammad Zulafif Rahim
zulafif@uthm.edu.my

Songlin Ding
songlin.ding@rmit.edu.au

Shoujin Sun
shoujin.sun@rmit.edu.au

[1] School of Aerospace, Mechanical and Manufacturing Engineering, RMIT University, Melbourne, VIC 3083, Australia

Keywords Polycrystalline diamond (PCD) · Electrical discharge machining (EDM) · Electrical discharge grinding (EDG) · Tool wear · Residual stress · Graphitization

1 Introduction

Advanced materials such as titanium alloys and carbon fiber-reinforced plastic (CFRP) have found wide applications in aviation industry owing to their excellent mechanical property, low weight-strength ratio, and high erosion resistance. However, titanium alloys are difficult to machine due to their low thermal conductivity and high chemical reactivity which adversely affect tool life, cause premature tool failure, and eventually lead to very low efficiency [1]. The recommended cutting speed for machining titanium alloys using high-speed steel (HSS) is over 30 m/min. This cutting speed can be increased to 60 m/min when adopting tungsten carbide (WC) tools [2]. However, when applied in high-speed cutting (larger than 100 m/min) in the finishing process, the tool life becomes unacceptably short: some tools can only last for a few minutes. With the progress in material science, polycrystalline diamond (PCD) has been gradually applied in industry to make high performance cutting tools. The significant hardness (over 8, 000 HV), low friction coefficient, and excellent thermo-conductivity of diamond of up to 500 W/mK at 300 °C make it one of the most promising tool material for machining titanium alloys and CFRP [3]. Experimental results have proven that PCD tools have much longer tool life than tungsten carbide tools in machining Ti6Al4V with the same cutting speed (100, 200, and 300 m/min) [4].

However, due to the extreme hardness, it is extremely difficult to grind PCD tools to shape, particularly when the work holding space is limited on small complex parts. Abrasive grinding and electrical discharge grinding (EDG), a variation

of electrical discharge machining (EDM) process but with a rotational electrode, are the two major methods utilized in industry to manufacture PCD tools. Conventionally abrasive grinding process provides high surface quality and a long tool life, but its machining efficiency is extremely low. EDG is a non-contact thermal erosion process in which the material is removed by a series of recurring electrical discharges between the electrode and the electrically conductive workpiece, in the presence of a dielectric fluid. Due to the different material removing mechanism of EDG and abrasive grinding, PCD tools manufactured with these methods are of different qualities and show different performances in machining titanium alloys.

Tso and Liu [5] found that PCD inserts fabricated by conventional grinding had longer tool life. In contrast, for EDG'ed tools, one of the problems encountered was the thermal residual stress which was caused by the mismatch of thermal expansion coefficient between diamond particles and cobalt [6, 7]. Residual stress within the PCD layer is generated in both sintering and grinding processes; its value indirectly affects the quality and performance of PCD tools [8]. According to Yahiaoui et al. [9], tensile residual stress in the PCD layer could cause inner cracks, weaken the strength of diamond to diamond bonding, and reduce tool wear resistance. It was assumed that the thickness of PCD layer influenced the distribution of residual stress in the entire PCD layer of an insert [10]. In other words, the distribution of residual stress depended on the thickness ratio of PCD layer and tungsten carbide substrate. Moreover, the size of PCD grains affected residual stress on PCD surface as well. Larger compressive residual stress existed within PCD layer made of bigger diamond particles (for example 30 μm) [11]. Another thermal defect after EDG process is graphitization. This will happen when temperature reaches 973 K with cobalt as its catalyzer, and this conversion is detrimental to tool quality because it weakens the strength of diamond and causes irreversible volume expansion [12, 13].

Cheng et al. had conducted comprehensive research in various types of wear in applying PCD tools and found that the development and modes of tool wear depended on the material of workpiece. The dominant tool wear mechanism in machining aluminum alloys tended to be abrasion and chipping caused by impurities on the grain boundaries, which led to severe edge rounding and significant flank wear, while, in cutting copper, the predominant tool wear was crater wear, which was related to an increase in temperature on the rake face. In the cutting of electroless plated nickel, micro-chipping of the cutting edge was significant. The chemical effect was predominant when machining steel [14]. For the machining of titanium alloy, the wear types are various and are affected by multiple factors. The cutting environment is severe due to its inherent property of low thermal conductivity. Furthermore, the element Ti is chemically active and has affinity to many tool materials [15, 16]. Cutting tools can be worn by abrasion, chemical erosion, diffusion, build-up edge (BUE), build-up layer (BUL), and other wear modes [17]. Based on the experiments of turning Ti6Al4V, Rosemar et al. [18] analyzed the wear mechanism and tool life of PCD tools. Severe crater wear and adhesion were found in the worn area, and it was assumed that these results could be attributed to the combination of attrition and diffusion–adhesion mechanism: adhesion wear occurred between the surfaces of workpiece and tool clearance face. Other studies also proved that high cutting temperature, which could exceed 800 K at cutting edge when the cutting speed was 190 m/min [19], accelerated the rate of chemical diffusion, and this process resulted in the formation of a titanium-carbide layer [20, 21]. Finally, this layer and some amount of tool material were removed by "plucking action," thus accelerated tool wear on the rake face. According to Cheng et al. [22], the high cutting temperature decreased the cohesive energy of carbon and weakened the C–C bond of diamond, which reduced the strength of the microstructure of diamond. In another research conducted by Amin et al. [23], a comparative experiment of milling titanium alloy Ti6Al4V with WC-Co and PCD tools, respectively, was carried out. The main wear mechanism of WC-Co tools generally included diffusion and superficial plastic deformation. Diffusion, abrasion, and notching were the main wear modes found on the surface of PCD tools. Honghua et al. [24] analyzed surface integrity and tool life by milling TA15 with PCD inserts. Their experimental results showed that value of flank wear (VB) increased by over 0.2 mm after 80 min when the cutting speed was 350 m/min. Adhesion and micro-chipping were found on PCD surface. The adhesion of tool material indicated a strong bond at tool/workpiece and tool/chip interface, this effect combined with a relatively high temperature reduced the yield strength of PCD tool and led to the development of nose wear and flank wear. Spalling was found on the surface of PCD cutting tools when the cutting speed increased to 375 m/min. The mechanism of PCD tool wear was mainly the interaction between adhesive wear and abrasive wear [25].

Although extensive research has been conducted to investigate the wear mechanism of PCD tools, the majority research is focused on the tool wear modes of conventionally ground PCD tools and how cutting parameters affected the development of tool wear. The wear mechanism and wear modes of PCD tools machined by EDG process are rarely investigated. Moreover, no thorough researches on the influence of invisible defects such as graphitization and large residual stress which may inflict sever damage to PCD tools in harsh machining conditions have ever been conducted.

This paper investigated the wear mechanisms and cutting performance of PCD tools machined with different methods and strategies. Wear resistance and cutting performance were examined by turning titanium alloy Ti6Al4V. To compare tool quality before and after the cutting tests, tool geometry,

Table 1 Basic physical properties of CTB010

Diamond grain size	Thermal conductivity	Thermal diffusion	Density	Diamond fraction	Cobalt fraction
10 μm	459 W/m K	0.24×10^{-3} m/s^2	4.08 g/cc	89.7 %	10.3 %

residual stress, and the level of graphitization were measured intermittently in each test. Different wears including flank wear, nose wear, and crater wear were investigated. The relationship between defects caused by tool manufacturing process and the evolution of wear was analyzed.

2 Experimental setup

2.1 Preparation of cutting tools

In this study, PCD inserts made of CTB010 (Element Six), which are widely used for metal works in manufacturing industry, were tested in turning titanium alloy Ti-6Al-4V. The basic physical property of the PCD is shown in Table 1. The inserts were prepared in two steps:

Step 1 PCD strips (3 mm in thickness) were wire-cut from a circular PCD disc; rectangular PCD inserts (7.0 mm × 7.0 mm) were made by further slicing the PCD strip (Fig. 1) into small inserts.

Step 2 PCD inserts were machined with two different methods: conventional abrasive grinding (CAG) and EDG.

Figure 2a, b shows the CAG and EDG processes, respectively. The conventional grinding was conducted on a computer numerical control (CNC) Diamond Grinder (COBORN RG6-FE). The grinding feed rate was 0.2 mm/min, and the grinding speed was 20 m/s. The EDG process was conducted with a commercial EDG machine (ANCA EDGe). To investigate the effects of different EDG parameters, two different EDG machining methods were adopted: a two-step method including a roughing and a finishing process and a three-step method which includes a roughing, a semi-finishing, and a finishing process. The roughing process is to achieve the highest machining efficiency by removing the workpiece material as fast as possible using large electric current and large in feed rate, while the finishing process is to maintain PCD surface quality by using small current and slow in feed rate to eliminate stressed and graphitized PCD structure. The detailed machine parameters are shown in Table 2.

The morphological parameters of PCD inserts after EDG and conventional grinding were examined with an Alicona (IF-EdgeMaster) optical microscope. As shown in Fig. 3, 3D images of each cutting tool were taken for further geometric analysis. The measurement of surface roughness, clearance angle, and radius of cutting edge was conducted by using software "Edge Master." The edge radii of PCD inserts machined with different methods are listed in Table 3. Before the cutting test, residual stress on the machined surface of each PCD insert was measured using PerkinElmer Raman Station 400F. Raman values were acquired with a 100-μm laser spot to analyze the types of carbon and residual stress on the machined surface.

2.2 Turning experiments

Figure 4 shows the equipment and the setup in turning of titanium alloy with PCD tools. The turning experiment was conducted on a CNC lathe (OKUMA GENOS L200E-M). A PCD insert was fasten on a tool holder which was clamped on

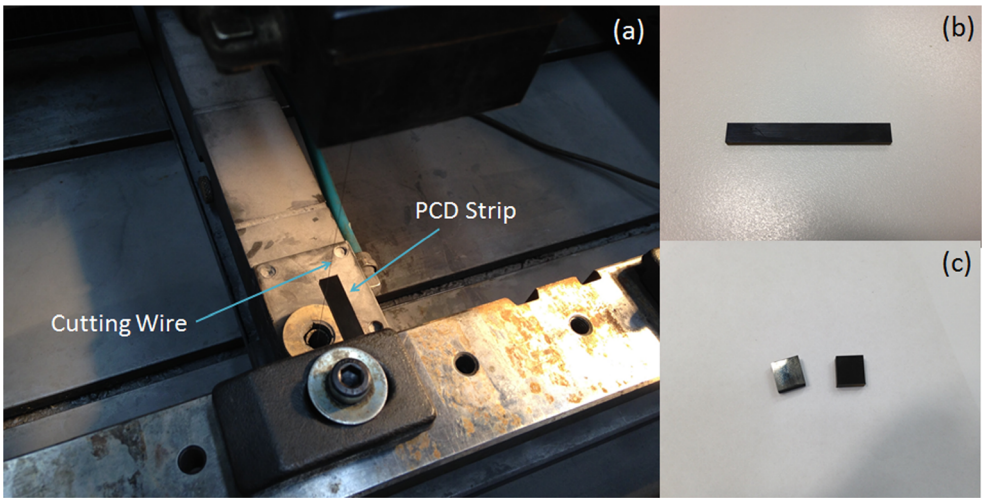

Fig. 1 **a** The Dophen wire-EDM machine. **b** A PCD strip (CTB010). **c** PCD inserts

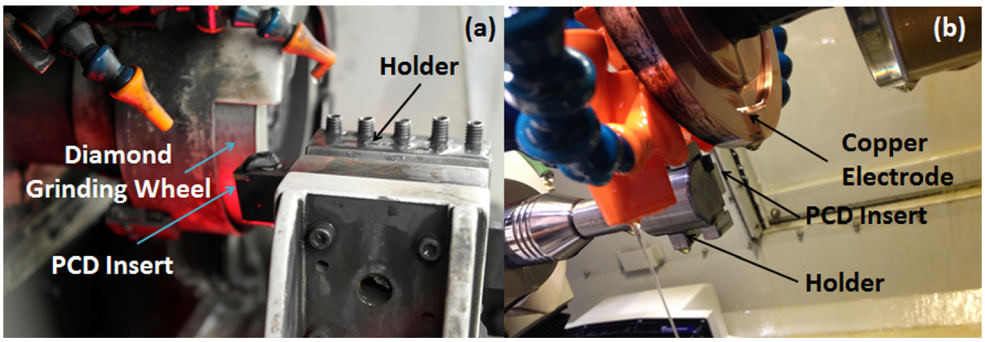

Fig. 2 **a** PCD inserts ground on the diamond grinder. **b** PCD inserts machined on ANCA EDGe grinder

a designed tool fixture (Fig. 4a). A dynamometer (PCB Piezotronics 260A01) was mounted on the base of the tool holder (Fig. 4b) for measuring the change of machining force during the cutting process. The dimension of the titanium alloy workpiece (Ti-6Al-4V grade 5) is 200 mm (L)×50 mm (D). Its basic physical properties and chemical composition are listed in Tables 4 and 5. The titanium alloy workpiece would be machined with three types of PCD inserts with same cutting parameters which were often used for the finishing process of turning Ti-6Al-4V [2]:

Cutting speed, 160 m/min (1,074 RPM)
Feed rate, 0.15 mm/rev
Cutting depth, 0.2 mm

Coolant of normal pressure was applied to reduce the cutting temperature. In order to check the evolution of tool wear, the morphology of each cutting tool was examined after turning consecutively for 1, 2, 3, and 4 min during the experiment. Tools would be rejected according to the following ISO3685 tool failure criteria: nose wear, VN=0.4 mm; average flank wear, VB=0.4 mm; notch wear, VC=0.6 mm; roughness of flank surface, R=1.6 μm; and any catastrophic fracture on cutting edge.

Cutting force was recorded by a force measurement system during the entire machining process. Force signal was recorded by a dynamometer as voltage signal and transferred to the laptop via an amplifier (PCB Piezotronics 480A22) and DAQ card (National Instrument 6036E), then processed by the software LabVIEW SignalExpress (Fig. 5b). The acquired voltage signals were filtered using the software MatLab (Fig. 5c) and converted into force values by multiplying the sensitivity of the dynamometer in each direction. The dynamometer could measure the forces exerted in three directions (Fig. 5a): feed force (X direction), back force (Y direction), and main cutting force (Z direction), which were the components of actual cutting force in the turning process.

Alicona optical microscopes and scanning electronic microscope (SEM) were utilized to check tool wear and surface quality after machining. Images of worn areas of workpieces and the elements of adhered materials were recorded so that the performance of cutting tools could be compared.

3 Experimental results and discussion

Tool wear and surface profile of the workpiece after being machined continuously for 1, 2, 3, and 4 min were recorded in the turning experiment. In general, wear modes such as flank wear, nose breaking, BUE, BUL, fracture, and cutting edge roundness which are caused by different mechanisms including mechanical, thermal, chemical, and possible electrical effects as predicted by Oosthuizen et al. were examined [2]. Residual stress and the phase of carbon after grinding were analyzed using the data from Raman spectrum.

3.1 Mechanism of flank wear

Flank wear reflects the friction between the workpiece surface and flank face of the cutting tool. Figure 6 shows the worn areas on the flank faces of three types of PCD tools after machining for 10 min. The acquired images (×50, Alicona EdgeMaster) show that flank wear on the tool surfaces was caused by the abrasion between PCD flank face and the surface of the workpiece. The most serious wear is found on the flank face of the conventionally ground insert. It can be seen in

Table 2 Machining parameters for two-step EDG and three-step EDG processes

Step	Two-step grinding (current/in feed)	Three-step grinding (current/in feed) (μm)
1	12A/150 μm	12A/150
2	1A/40 μm	4A/40
3		1A/30

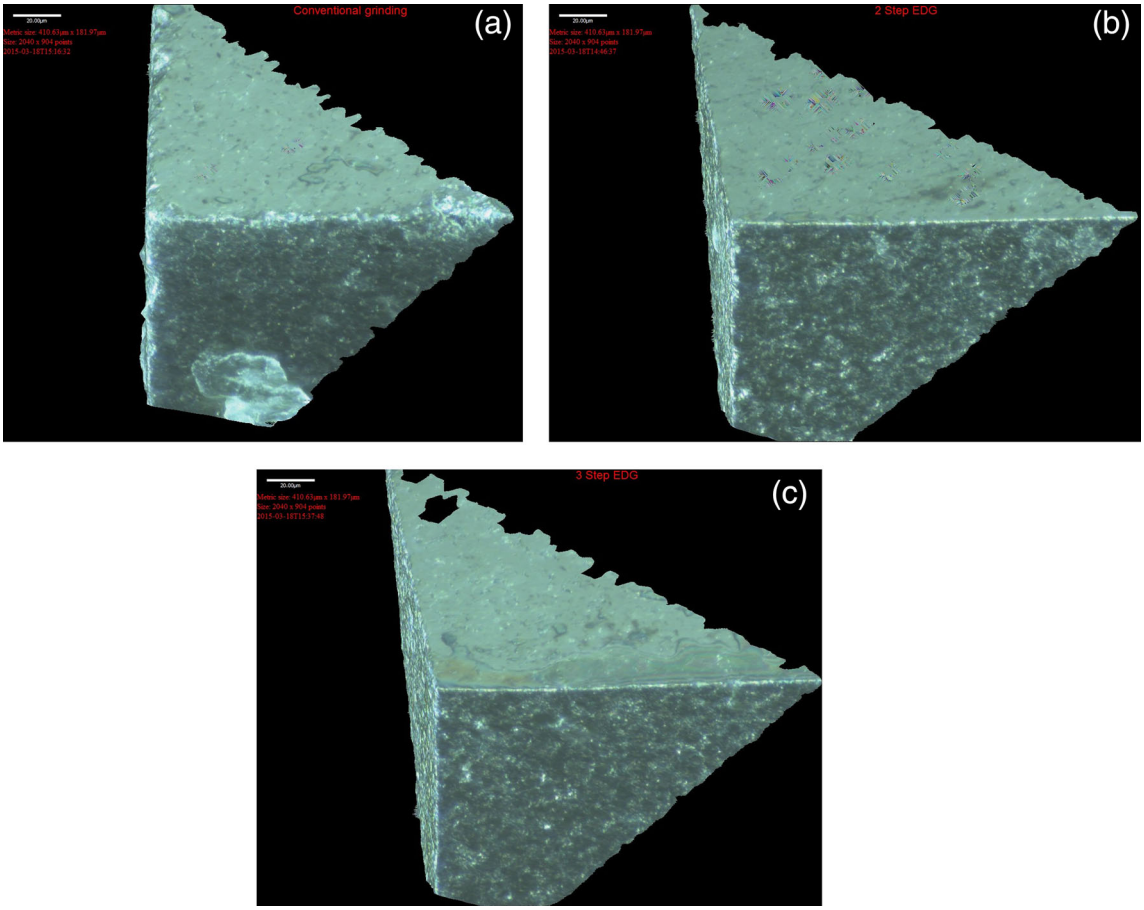

Fig. 3 3D images (×50) of tool nose and cutting edge machined with conventional grinding and EDG. **a** Conventional grinding. **b** Two-step EDG. **c** Three-step EDG

Fig. 6a–d that tool wear developed from a narrow area around cutting edge into a large triangular area. For the PCD tool manufactured with the two-step EDG process (Fig. 6e–h), the trend of tool wear development was similar to that of the abrasively ground PCD insert but with a much smaller abrasive area which indicated that the tool–workpiece contact area was small. Also, it can be seen that the length of nose wear was just a half of that of conventionally ground insert, which means that tool wear rate at this area was smaller during machining. In contrast, tool wear resistance of the PCD tools machined with the three-step EDG process was better than the tools machined with other two methods: the initial length of flank wear was smaller (Fig. 6i) and the worn surface was limited to the area around the cutting edge, not much PCD material near the tool nose was removed in the entire cutting process (Fig. 6i–l).

Table 3 Cutting edge radius of three PCD inserts after machining

Machining methods	Cutting edge radius (μm)
Conventionally ground	5.6
2-step EDG	4.18
3-step EDG	3.22

The change of VB values and main cutting force (*Z* direction) reflects the evolution of flank wear of different PCD inserts. According to Fig. 7a, the VB values of all the inserts, measured at the position about 100 μm away from tool nose, were around 50 μm (after 1 min) and developed in different rates in the following 9-min turning. To be specific, conventionally ground PCD have the most serious flank wear rate, the increase of VB showed a linear trend during the machining. After 10 min, its VB reached near 320 μm which was the largest among all the three tools. The evolution of flank wear of the tool machined with the two-step EDG method has a similar trend but not as severe as the conventionally ground insert. Its VB starts at 35.6 μm after 1 min, which was the lowest among all three tools, increased to 220.47 μm linearly after 10 min. Also, the VB of the two-step EDG'ed insert after 10-min is similar to that of conventionally ground one after 6 min. It is shown that the tool machined with the two-step EDG process has a better flank wear resistance than the conventionally ground PCD tool. The smallest VB after 10 min was obtained by using the three-step EDG'ed PCD insert. Its wear curve was similar to the standard wear trend which includes an initiation, a steady, and a severe wear process. After 10 min, a VB of 117.04 μm was achieved. This was the lowest value and indicated the best wear resistance

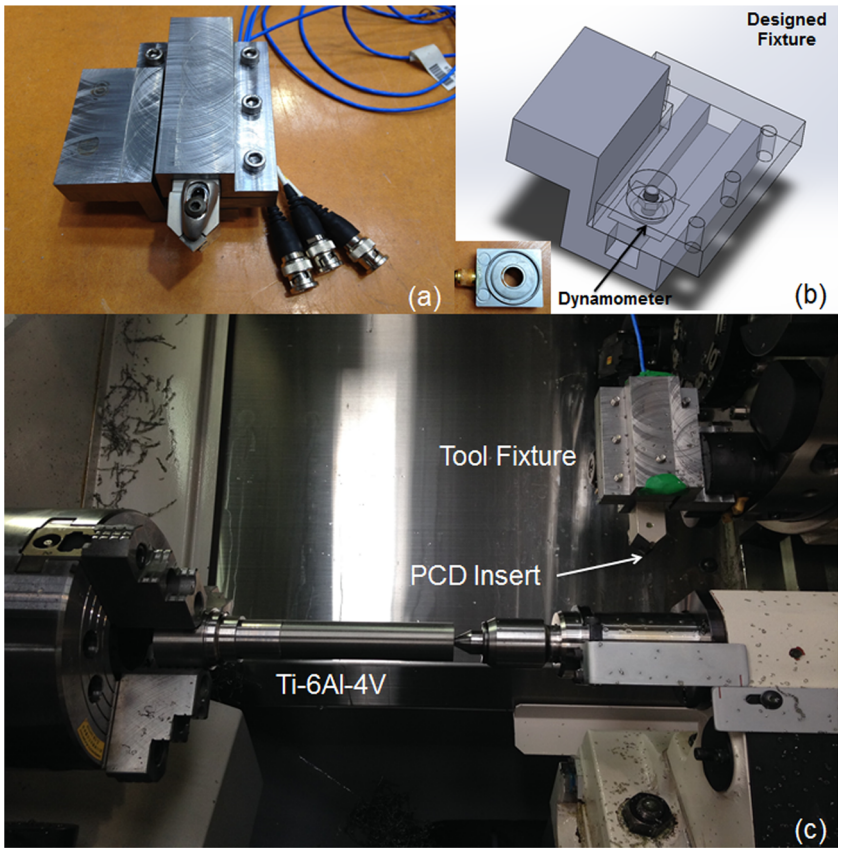

Fig. 4 Equipment used in the turning experiment. **a** Assembled tool fixture. **b** 3D model of the designed fixture. **c** Experimental setup of the turning test

of this type of tool. The component of cutting force in *Z* direction reflects the difference in the development of flank wear as well. Generally, the change of *Z* direction force has the similar trend as that of VB values for each PCD insert (Fig. 7b). As flank wear is caused by the tool/workpiece abrasion, the increase of friction area leads to the raising of cutting force in *Z* direction. All the forces initiated around 100 N and went up to different values during the cutting process. Largest cutting force was found when turning Ti6Al4V with the CAG'ed PCD insert (293 N after 10-min turning), and the force in turning the alloy with the two-step EDG'ed tool was smaller (215 N after 10-min turning) but had a similar trend. In contrast, the variation of cutting force in *Z* direction with the three-step EDG'ed insert was not obvious, which were 119, 136, 146, and 161 N, respectively, in each step of the experiment, there conformed to the change of VB values on the flank face of the three-step EDG'ed insert.

As shown in Fig. 6l, obvious notch wear was formed at the end of flank wear area on the flank surface of the three-step EDG'ed insert, while this was not found when turning with the conventionally ground PCD tool and the tool machined with the two-step EDG process. SEM images of regions near the tool nose (Fig. 8) show more detailed information about the flank wear. It can be seen that material adhered to the worn flank face, some of them was removed by abrasion and attrition, and fresh PCD surface was exposed and led to further wear process. Results of energy-dispersive X-ray spectrum (EDS) analysis (Fig. 9) show that the accumulated material is titanium alloy. This indicates that serious diffusive-abrasive wear happened in this area. The adhesion of titanium was the main factor that contributed to flank wear. According to the theory of Bhaumik et al. [26], adhesion happened frequently when there was chemical affinity between workpiece and tool surface. This caused further material diffusion between the workpiece and cutting tools. Because of the feeding movement of the cutting tools, high temperature and high compressive stress were generated between the surface of workpiece and flank surface which accelerated the diffusion and attrition process [27]. Although the temperature on flank face was lower than the temperature on clearance face, abrasion on flank face was constant and lasted longer, and the constant and long time contact provided sufficient time for diffusive-abrasive reaction. Also, PCD is sensitive to high temperature, and around 36 % of its hardness can be reduced when machining

Table 4 Basic physical properties of Ti-6Al-4V

Material	Density	Hardness	Elastic modulus	Poisson's ratio	Thermal conductivity
Ti-6Al-4V	4.43 g/cc	349	113.8 GPa	0.342	6.7 W/m K

Table 5 Basic chemical composition of Ti-6Al-4V

Ti	Al	V	Fe	C	O	N	H
88.3 %	6.5 %	4.3 %	0.3 %	0.1 %	0.3 %	0.05 %	0.02 %

temperature rises from 300 to 500 K [28]. Even though coolant was applied in the machining, the instantaneous temperature near the cutting edge and tool nose was still high enough to weaken the diamond structure on flank face. As a result, flank wear was formed and developed by the continuous cycle of adhesion, diffusion, and the removal of this layer. Especially, when compared with EDG'ed inserts, abrasion between the cutting tool and workpiece was more severe because more adhered titanium within worn area of conventionally ground PCD was removed.

3.2 Tool nose wear analysis

As the landing area of flank wear, nose wear rate is generally higher than flank wear rate [29]. It was found that different degrees of nose wear occurred after 10-min turning (Fig. 10). To be specific, CAG'ed tools suffered most serious tool nose wear (Fig. 10a), and the worn area extended nearly to the boundary between PCD layer and the WC substrate. For the two-step EDG'ed tools (Fig. 10b), the mass loss around tool nose is less than that of conventionally ground tools, and the worn area near the tool nose of three-step EDG'ed insert is smallest (Fig. 10c), which means that EDG'ed tools have better nose wear resistance than the conventionally ground tools.

In Fig. 8, notching near tool nose is found along the secondary cutting edge of all three samples as well. On a cutting tool, tool nose suffers the maximum cutting temperature which might cause thermal softening of material if it is high enough. Sreejith et al. [30] proved that notching near tool nose was produced by the oxidation wear combined with high temperature. From the result of EDS analysis at the notching area (Fig. 11), titanium and oxygen present at worn area. This indicates that chemical reaction between titanium alloy, carbon, and oxygen contributed

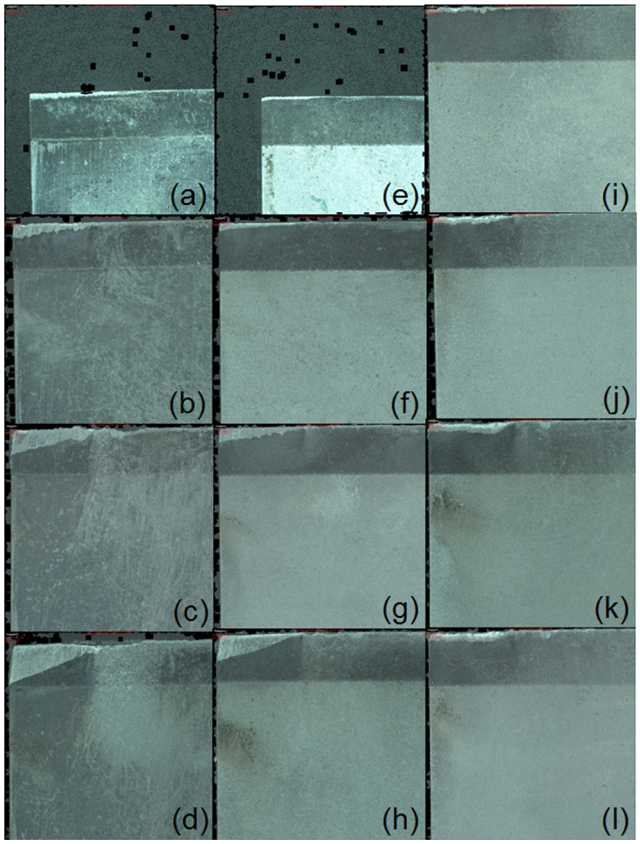

Fig. 6 Intermittent images of flank wear on tools manufactured with different methods. **a** CG tool after 1 min. **b** CG tool after 3 min. **c** CG tool after 6 min. **d** CG tool after 10 min. **e** Two-step EDG'ed tool after 1 min. **f** Two-step EDG'ed tool after 3 min. **g** Two-step EDG'ed tool 6 min. **h** Two-step EDG'ed tool 10 min. **i** Three-step EDG'ed tool after 1 min. **j** Three-step EDG'ed tool after 3 min. **k** Three-step EDG'ed tool after 6 min. **l** Three-step EDG'ed tool after 10 min

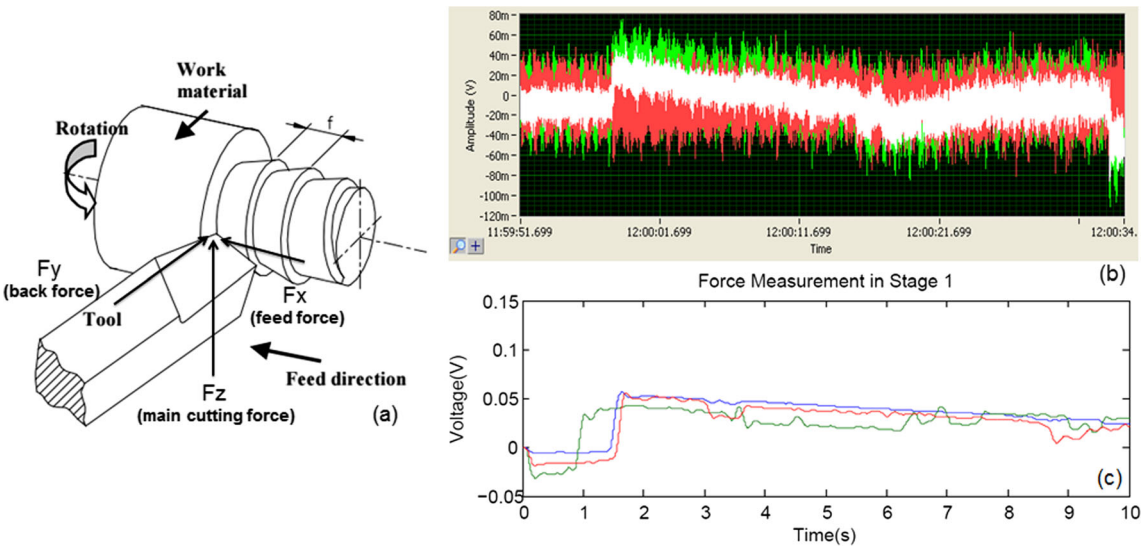

Fig. 5 **a** Cutting force model of turning [14]. **b** Force signal acquired by the software "LabVIEW SignalExpress." **c** Force signals filtered by "MatLab"

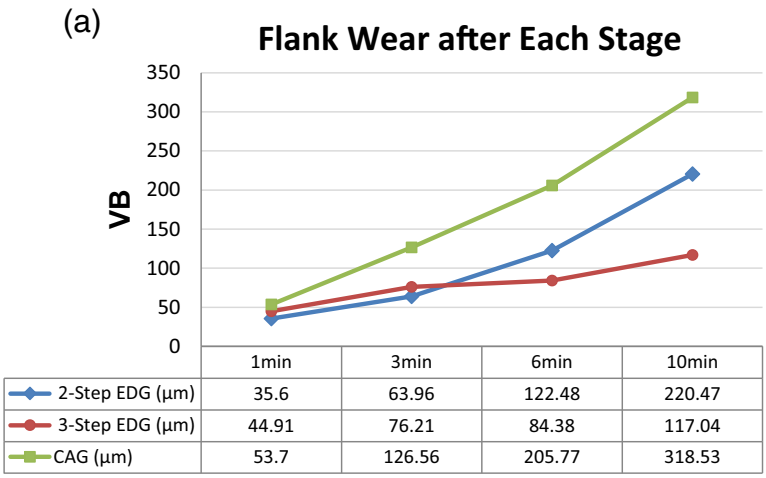

	1min	3min	6min	10min
2-Step EDG (μm)	35.6	63.96	122.48	220.47
3-Step EDG (μm)	44.91	76.21	84.38	117.04
CAG (μm)	53.7	126.56	205.77	318.53

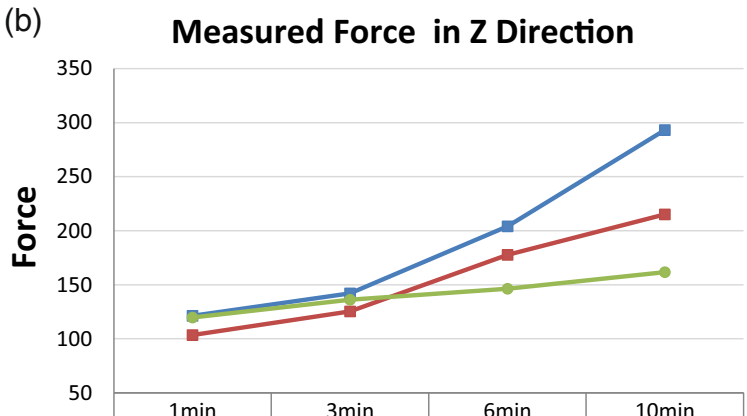

	1min	3min	6min	10min
CAG (N)	121.2436	142.1134	204.12652	293.171
2-Step EDG (N)	103.3552	125.2188	177.69144	215.05832
3-Step EDG (N)	119.65352	136.1506	146.28736	161.59188

Fig. 7 **a** VB values of different inserts in each stage of experiment. **b** Force in *Z* direction in each step of turning experiment

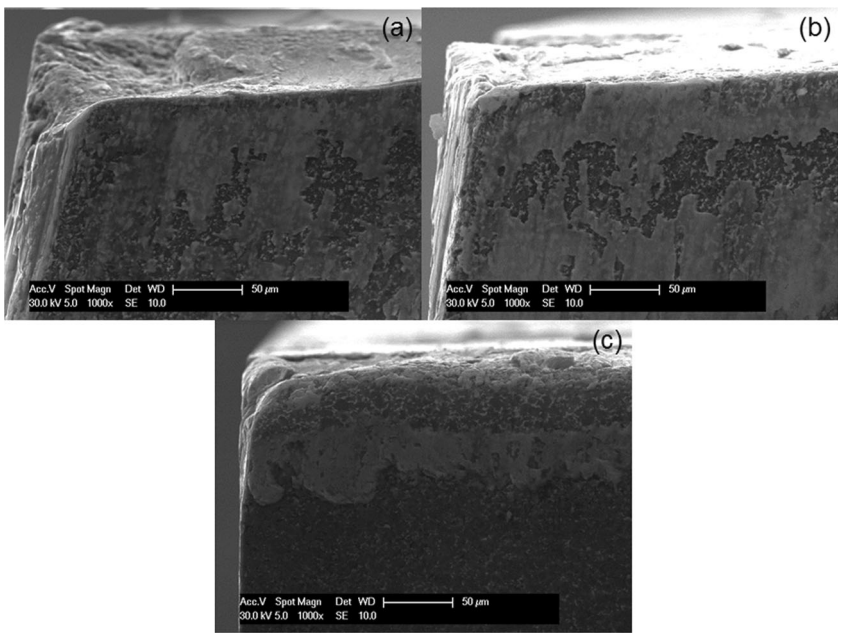

Fig. 8 SEM images (×1,000) of rake flank face after 10-min turning. **a** CAG'ed tool. **b** two-step EDG'ed tool. **c** Three-step EDG'ed tool

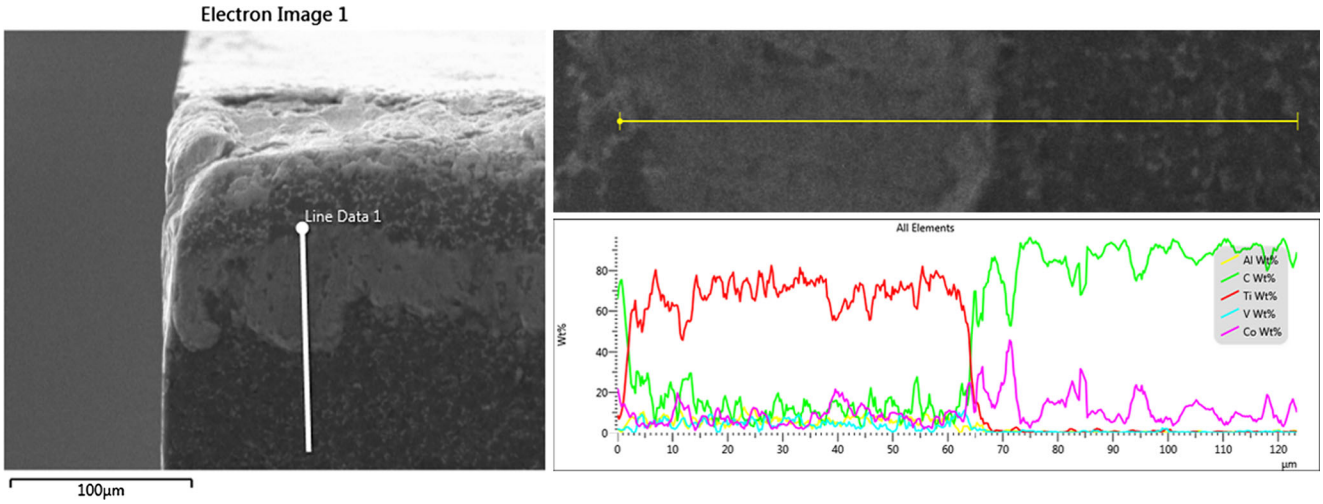

Fig. 9 EDS analysis of elements accumulated on worn flank surface of three-step EDG'ed tool after 10-min turning

to notching around the tool nose. Also, this phenomenon proved that the temperature at the tool nose was very high, although coolant was applied in the turning process.

As shown in Fig. 12a, the change of nose wear shows similar trend as that of flank wear. Specifically, the values of VN of all three inserts start at nearly the same value (around 50 µm). The worst result was acquired by using conventionally ground PCD with a VN value reaching nearly 400 µm, which was the biggest one. In contrast, the VBs of the two-step EDG'ed insert were 71 µm (after 3 min), 140 µm (after 6 min), and 250 µm (after 10 min). The tool machined with the three-step EDG process showed the best wear resistance, the trend of wear development was steady, and it was only 87.14 µm after 10-min turning, which was even smaller than the maximum value of flank wear. It was also found that, in the conventionally ground and two-step EDG'ed PCD inserts, the development of wear around tool nose was faster than on the flank face, which indicates more abrasive reaction occurred near tool nose in turning titanium alloy. However, in the three-step EDG'ed PCD insert, the VBs grew more rapidly than the VNs, showing a better wear resistance at tool nose than on flank face.

The development of tool nose wear led to the change of cutting force in *Y* direction (Fig. 12b) and affected the profile of machined surface at the same time. It is known that peaks and grooves were generated by the successive movements of tool nose at intervals of feeds [31]. Therefore, the examination of surface profile is able to provide important information about tool wear: the fracture of tool nose during turning causes the variation of cutting force and continuously causes continuous changes in the depth of grooves on the workpiece surface. According to Fig. 12b, the cutting force in *Y* direction increased significantly when turning workpiece with both CAG'ed PCD tool and two-step EDG'ed tool. This is reflected by the decreasing of the groove depth after 10-min machining

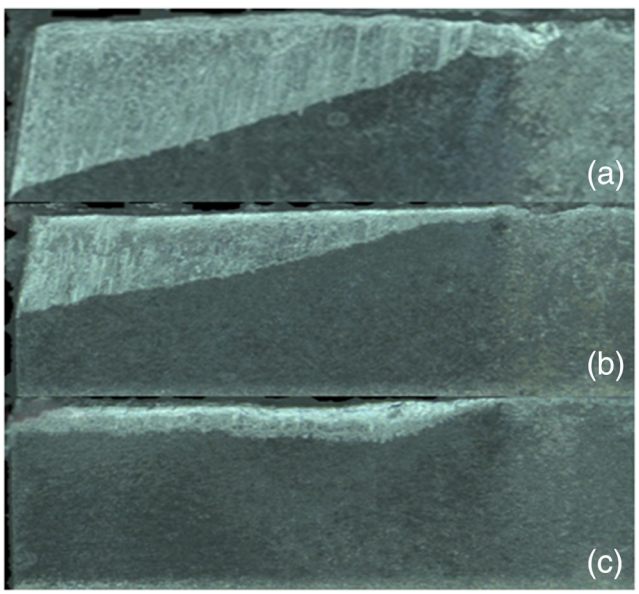

Fig. 10 Enlarged images of flank face after 10-min turning (×50, "Alicona," EdgeMaster). **a** CAG'ed tool. **b** Two-step EDG'ed tool. **c** Three-step EDG'ed tool

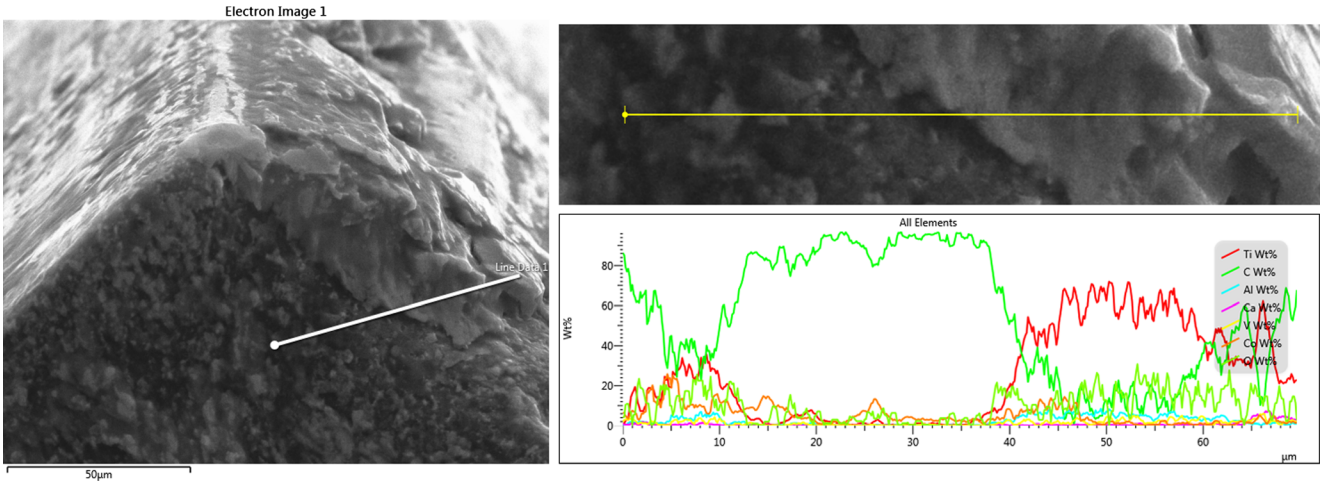

Fig. 11 EDS analysis of elements composited on worn clearance surface of conventionally ground insert after 10-min turning

(Figs. 13b, c and 14b, c). Compared with the groove depth achieved in the 1-min machining, there was a decrease of around 20 µm. This was caused by the material lose on the CAG'ed PCD tool nose which led to larger force in *Y* direction in removing workpiece material. However, for the grooves machined by the three-step EDG'ed insert, it decreased less than that of machined by the CAG'ed insert: the depth was kept around 100 µm (Figs. 13a and 14a), which meant a

Fig. 12 **a** Values of VN (tool nose wear) after each step of turning experiment. **b** Force in *Y* direction in each step of turning experiment

(a)

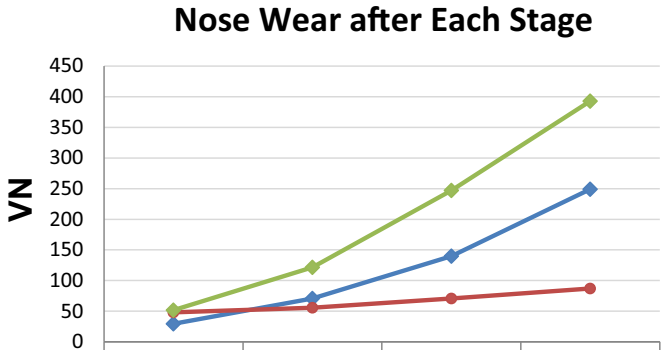

	1min	3min	6min	10min
2-Step EDG (µm)	29.6	70.77	139.94	249.05
3-Step EDG (µm)	48.02	55.51	70.88	87.14
CAG (µm)	51.7	121.61	247.25	392.67

(b)

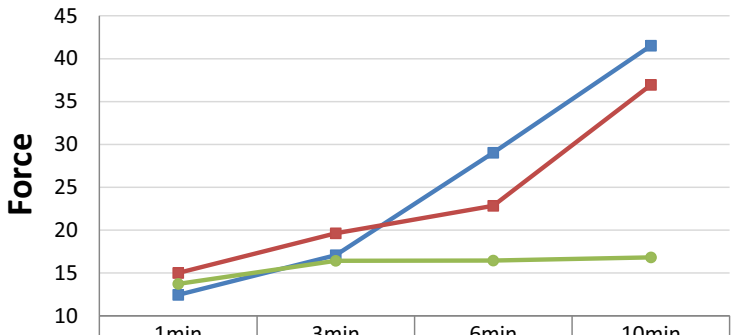

	1min	3min	6min	10min
CAG (N)	12.44061	17.07797	29.02809	41.51329
2-Step EDG (N)	14.99408	19.63144	22.84192	36.9442
3-Step EDG (N)	13.73372	16.40912	16.45371	16.81043

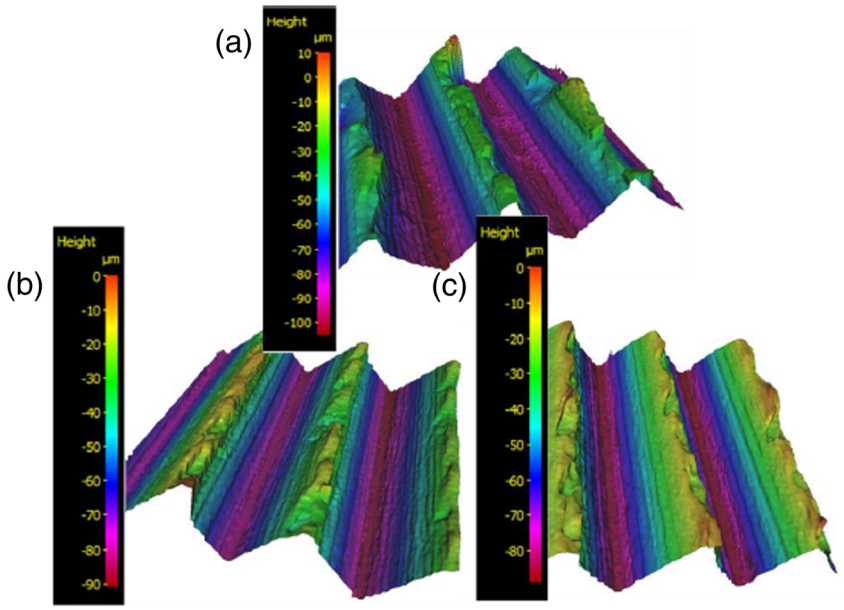

Fig. 13 Depth of workpiece surface after 1-min turning by **a** three-step EDG'ed tool, **b** two-step EDG'ed tool, and **c** conventionally ground tool

relatively intact tool nose was retained. The change of back force (*Y* direction) proved this assumption as well. The back force for the first minute cutting was around 12 N and increased only 5 N during the following 9-min cutting. This meant its tool nose was sharp enough and no increase in cutting force was caused in the following cutting process.

3.3 Crater wear analysis

It is known that PCD has high resistance to crater wear under normal cooling condition. However, tool wear was found after 10-min turning on the rake face of all cutting tools. Figure 15 illustrates the tool wear on rake surface and cutting edge of each PCD insert. It is clear that the level of cutting edge blunt and crater wear on the rake face are different among the three types of PCD tools. The cutting edge becomes blunt owing to the loss of tool material on the rake face near the cutting edge (Fig. 15d, g, and i). It can been seen in the SEM images that severe crater wear occurred in the 10-min turning process: there was titanium adhesion near cutting edge and a "hollow area" near the worn cutting edge of the CAG'ed tool (Fig. 8a). It has been proved that this type of wear is generated by chemical diffusion at tool/chip interface [1]. It is thermally activated and developed by removing the adhesive material by plucking action. The worn profile of the conventionally ground PCD surface was similar to that found by Rosemar et al. [15]. Also, because the rate of chemical diffusion and adhesion depends on the temperature at tool/chip interface [27], it is reasonable to assume that the temperature at the

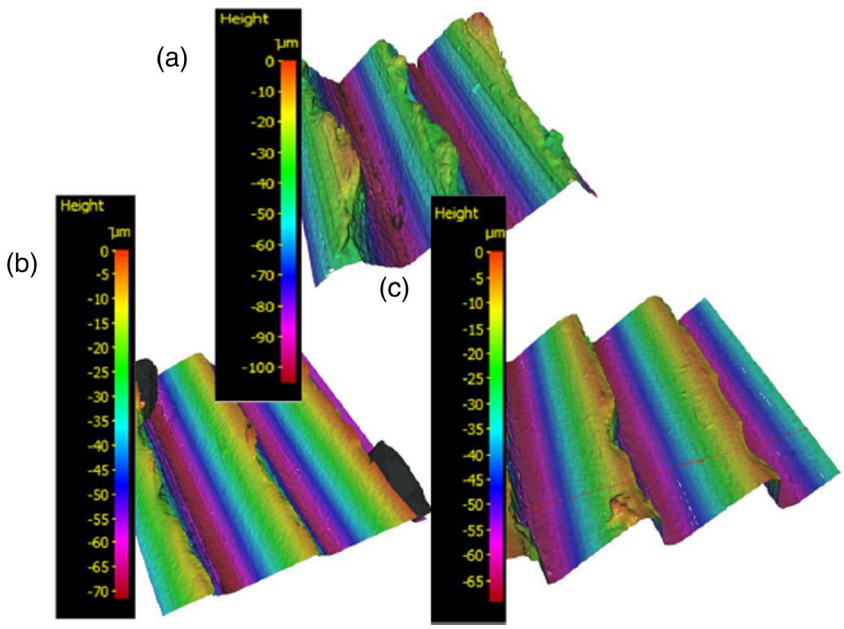

Fig. 14 Depth of workpiece surface after 10-min turning by **a** three-step EDG'ed tool, **b** two-step EDG'ed tool, and **c** conventionally ground tool

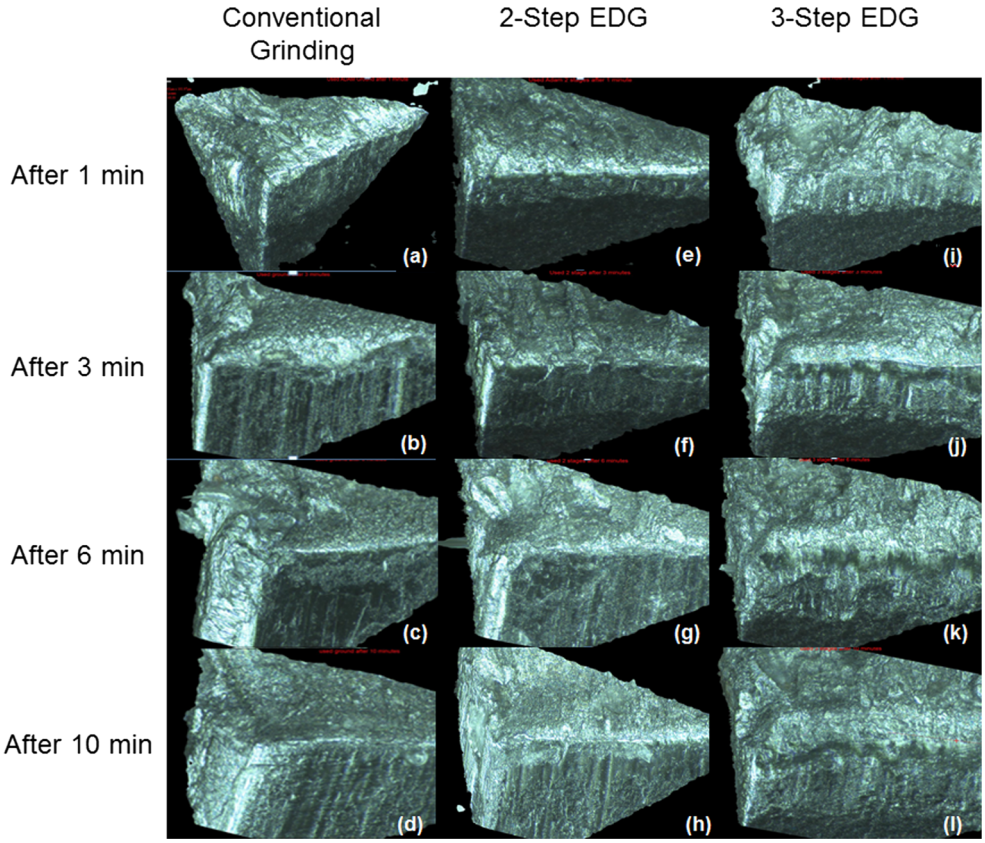

Fig. 15 Wear on tool nose and cutting edge after each step of turning experiment ("Alicona" EdgeMaster ×50)

worn area was higher and the chemical reaction was severe in turning titanium with conventionally ground PCD tools. However, different from conventionally ground tool, crater wear of EDG'ed tools was less serious in the 10-min machining.

Figure 15 shows that the large area of BUL and BUE on the cutting tools particularly the tool ground with the three-step EDG method. A thick titanium alloy layer was formed after 3-min turning, and this layer became even larger when the experiment was finished (Figs. 15j–l and 16). BUL was formed on the rake surfaces, and this was the cause that led to the decrease in the development of wear on their rake faces. As aforementioned, the development of diffusive-adhesive wear depends on the temperature at the tool/chip interface. During the turning process, the thermal effect caused by the deformation and friction at tool/chip interface was small, and this could be proven by the shape of chips (Fig. 17). Compared to the chips generated by conventionally ground inserts which were twisted together, the chips created by EDG'ed PCD inserts were regular and the radii of curves were smaller. Especially for the three-step EDG'ed PCD inserts, the chips were segmented during 10-min machining. The curvature of chips represents the tool-chip length, it is an important parameter which contains information about the contact between chip and rake face. A shorter tool-chip contact led to better coolant penetration [15]. According to Minton et al. [32], the temperature at tool/chip interface is over 1,300 K in dry cutting; therefore, applying coolant is necessary when PCD tool is used because the high temperature can accelerate diffusive-adhesive process and deteriorate the strength of PCD tools [24]. The adhered titanium alloy on the rake face of the three-step EDG'ed insert means that only a part of BUL was softened and removed, and leaving most part of BUL adhered on rake surface because the cutting temperature was lower than when the other two types of PCD tools were applied. As a result, the residual BUL left on the rake face stopped the further development of crater wear, preserving an intact rake surface on the EDG'ed insert [20]. This can be proved by the wear at tool nose and its cutting edge. It can be seen that, on the EDG'ed PCD inserts, the cutting edge near tool nose was well kept and abraded titanium could be found on nearby surfaces (Fig. 16b, c). On the other hand, the edge of conventionally ground tool along nose direction was abraded seriously; a blunt edge with large nose radius was found after the entire turning process was completed (Figs. 15d and 16a).

Furthermore, relative temperature of each tool can be indirectly predicted based on the profile of peaks and grooves shown in Fig. 18. The shape of grooves machined by the conventionally ground tool (Fig. 18c) was non-uniform after 10-min machining: titanium alloy was "squeezed" along the direction of feed. In contrast, the profiles of the groove machined by the three-step EDG'ed tool (Fig. 18b) and the two-step EDG'ed PCD tool (Fig. 18a) were still symmetric. According to Oosthuizen et al. [2], the temperature on tool face was over 1,000 K. Although coolant was applied, the

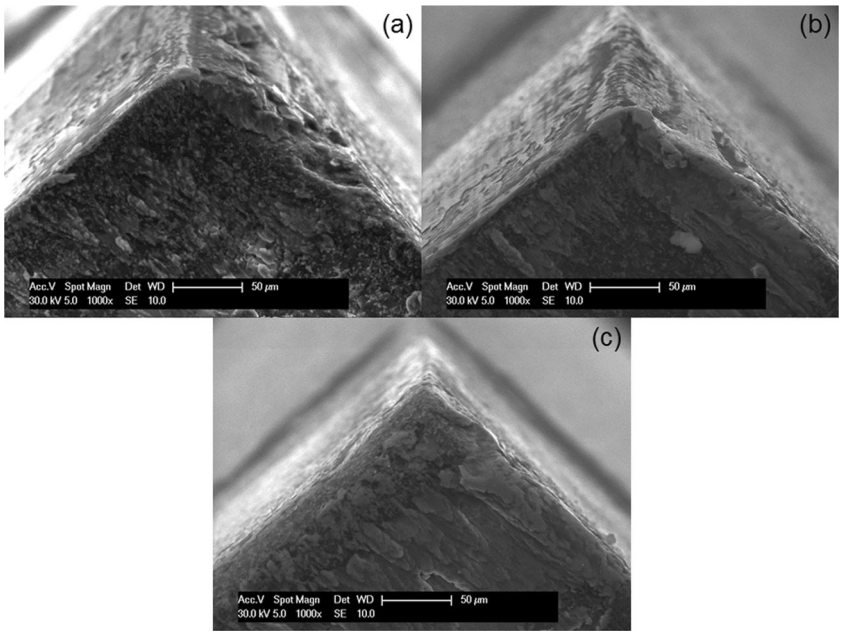

Fig. 16 SEM images of rake face after 10-min turning. **a** CG tool. **b** Two-step EDG'ed tool. **c** Three-step EDG'ed tool

temperature around tool nose was high enough to soften the workpiece material. Therefore, this phenomenon was because the material at tool/chip interface and tool/workpiece interface which was softened at high temperature at tool/workpiece interface was moved along with cutting tools under the force in the feed direction. The asymmetric profiles of surfaces machined by conventionally ground tools proved that the temperature was higher than those of EDG'ed tools. High temperature caused by friction and large feed force accelerated the diffusive-abrasive process and led to larger wear areas on flank face and rake face of the conventionally ground tool. From the profiles of EDG'ed tools, it can be predicted that the temperature around EDG'ed tool nose areas was not as high as that at conventionally ground tool nose. Moreover, a thicker layer of workpiece material adhered to the tool surface and tool nose, and this prevented the direct contact between PCD and high temperature workpiece material. Thus, the adhered layer reduced the area of worn surface and preserved intact tool noses of EDG'ed tools during the turning process.

3.4 Effects of residual stress and graphitization

Based on the discussion in Section 3.1, it is found that PCD tool machined by the three-step EDG process has the best wear resistance. It ended up with the lowest VB and VC after 10-min turning. For EDG'ed and conventionally ground PCD

Fig. 17 Chips after 10-min turning. **a** CG tool. **b** Two-step EDG'ed tool. **c** Three-step EDG'ed tool

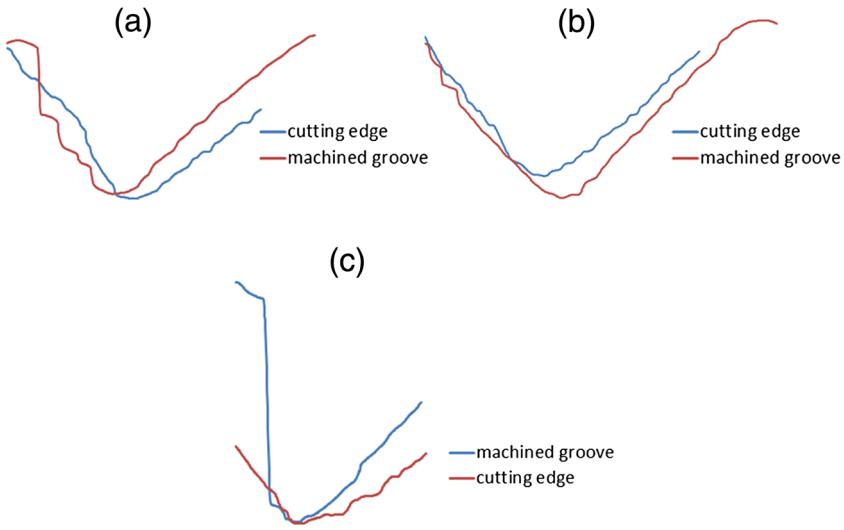

Fig. 18 Profiles of cutting edges and machined grooves after 10-min turning. **a** Two-step EDG. **b** Three-step EDG. **c** Conventionally ground

tools, the difference in quality does not exist only in surface roughness and the sharpness of cutting edge but also in the residual stress on the tool surface.

To analyze the residual stress, Raman spectrum of each PCD insert was measured before the cutting test. The shift of Raman value stands for the existence of residual stress on PCD surface. The results (Fig. 19) show that that both abrasive grinding and EDG were able to ease the compressive condition of residual stress on the PCD layer. Furthermore, from the Raman spectrum of each tool, graphite was detected to exist on the machined surface. The peak of graphite was higher for both EDG machined tools in comparison to that of the conventionally ground PCD surface (Fig. 19).

For each PCD tool, the value of Raman shift was measured three times, and the average values of recorded data were used for calculating the residual stress in PCD layer. The calculation of residual stress is based on the following equation [33]:

$$\sigma = -(\mathrm{vs}-\mathrm{vr})/\chi \quad (1)$$

where σ is the residual stress (positive means compress stress, negative means tensile stress), vs is the measured Raman shift value of the diamond, vr is the unstressed Raman value (1,330/cm), and χ is the coefficient of stress-induced frequency shift (1.98 GPa/cm).

Figure 20 shows the Raman shift value obtained from the PCD inserts. Tensile residual stress of 3.01 and 1.71 GPa was found on the two-step and three-step eroded PCD tools, respectively. On the other hand, compressive residual stress of 0.54 GPa was found dominating the surface of conventionally ground PCD tools. By comparing the performance of two-step and three-step eroded PCD tools, it was found that the residual stress significantly affected tool performance. In this study, PCD tools machined with three-step EDG process had lower residual stress and had achieved 1.5 times better wear resistance (considering the flank wear) than the two-step PCD after 10 min in the turning process. Because residual stress exists at cobalt/diamond interface, the strength at this area is weak. Residual stress with a big value favors crack propagation in grain boundaries and leads to diamond

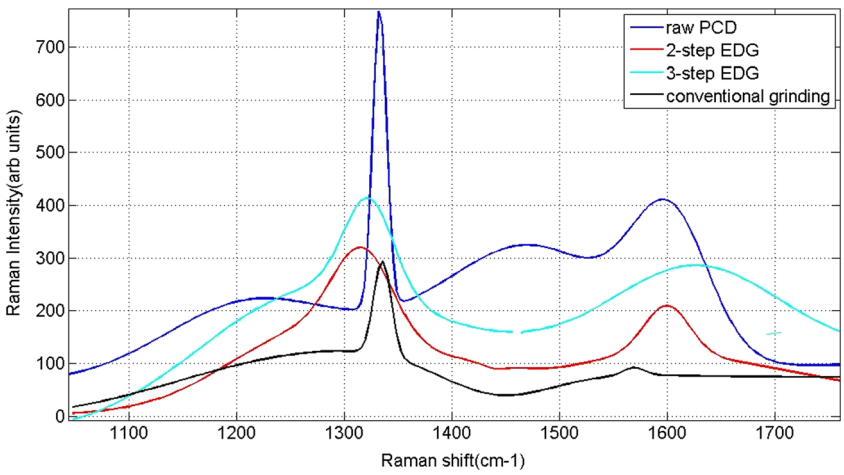

Fig. 19 Results of Raman spectrum on flank surface of three PCD inserts after filtering

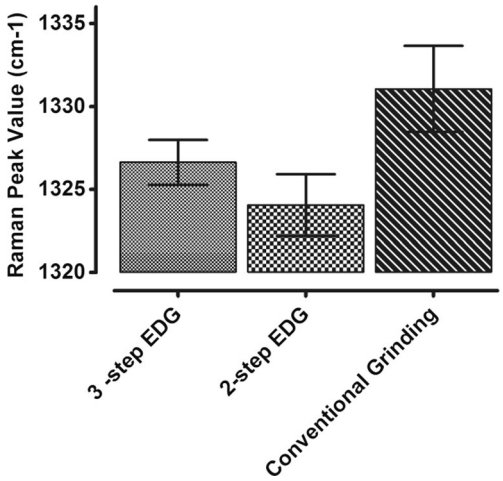

Fig. 20 Raman peaks of the PCD surface of three PCD inserts

grain decohesion. This weakened structure reduces the abrasion resistance of machined surface. Under the impact of extrinsic constant loading, material near cobalt/diamond interface worn away first and some intergranular cracks are produced [34]. As a result, bigger value of residual stress caused more unstable structure within the PCD layer.

According to Fig. 19, it can be seen that different carbon phases including graphite (around 1,600/cm), polycrystalline diamond (1,330/cm), and nano-crystalline diamond (around 1,250/cm) were found on machined PCD surfaces. Nano-sized diamond was found in the layer of conventionally ground PCD, while this structure did not exist in the PCD manufactured with EDG process. In conventional grinding, exerted shear stress and compression did not affect the existence of the nano diamond particles. However, in the EDG process, due to the thermal effect generated by plasma, nano diamond particles were converted to graphite and were removed in the machining. Yingfei et al. [35] found that diamond-graphite conversion was one of the reasons causing diffusive tool wear on flank face. The quantity of graphite can affect the strength of PCD structure and reduce its abrasion resistance as well. The peaks of graphite in Fig. 18 show the graphitization in tools machined by the two EDG processes. In the turning process, graphite on the top surface was removed by the abrasion, and the underneath layer of graphite weakened the strength of cutting edge and tool nose and accelerated the fracture and material loss in these areas.

Different from PCD tools machined by the EDG process, residual stress in the conventionally ground PCD tools was compressive, and the level of graphitization was the lowest. However, the tool performance of conventionally ground PCD was the worst among all the tools. Figure 21 presents the condition of tool nose after 20-s turning which indicated the initiation of tool wear. In Section 3.2, it was found that there was obvious material loss at the nose in the conventionally ground PCD tool, while the tool noses of the EDG'ed inserts were relatively intact and workpiece material adhered around tool noses. The appearance of significant fracture mode at the early machining step is a good indication of the occurrence of internal cracks that typically associated with the grinding process. The micro-cracks caused by the compressive stress initiated the wear on flank face and tool nose, and these defects accelerated the development of fracture, which led to the development of tool wear.

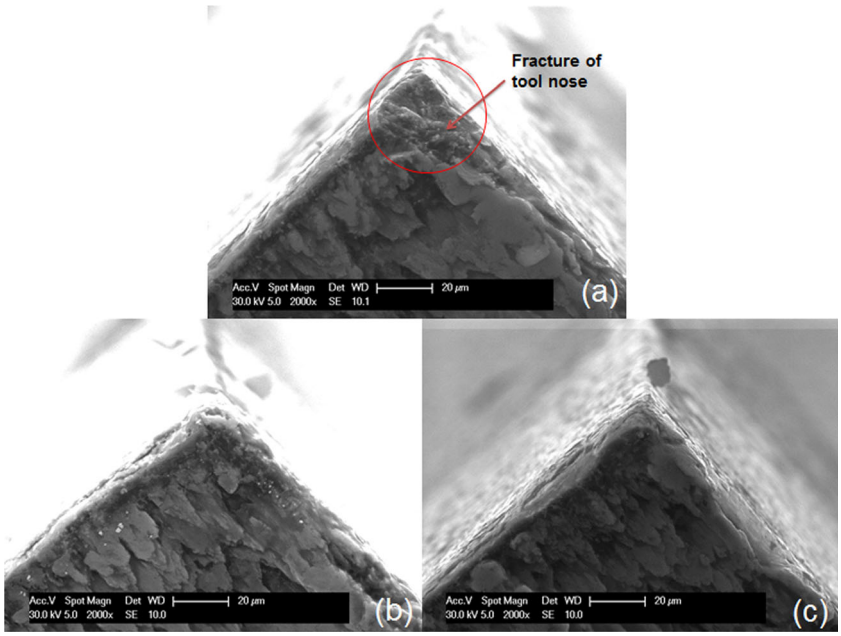

Fig. 21 SEM images (×2,000) of tool nose after 20-s turning. **a** Conventionally grinding tool. **b** Two-step EDG'ed tool. **c** Three-step EDG'ed tool

4 Conclusion

Different levels of tool wear were found in PCD tools manufactured with conventional abrasive grinding, two-step, and three-step EDG processes. The wear included flank wear, tool nose wear, crater wear, and edge chipping.

Conventionally ground PCD suffered the most serious tool wear among all three types of PCD tools. In contrast, the least worn was found on flank face, rake face, and cutting edges of the tools machined with the three-step EDG process.

Flank wear of PCD tools was caused by chemical diffusion and abrasion between tool surface and workpiece in turning titanium alloy which was activated by the high temperature at tool/workpiece interface. The largest VB and VC which were found on the surface of the conventionally ground PCD tool indicated that its cutting temperature was highest in the machining. The size of worn areas on rake surface also proved that higher tool temperature led to more serious crater wear. Among all three types of PCD inserts, conventionally ground PCD inserts generated the highest temperature during turning. This accelerated the development of tool wear and increased cutting temperature in return.

By analyzing surface profile of the grooves cut by the three types of PCD tools, it was found that there was an obvious decrease in the depth of grooves cut with conventional ground PCD tool and the tool ground with the two-step EDG method. This phenomenon proved that the wear at tool nose of these two tools was more serious than that of the tools ground with the three-step EDG method. The temperature at tool/workpiece interface of conventionally ground and two-step EDG'ed inserts was highest as proved by the asymmetric profile of the grooves.

Residual stress and graphitization were investigated through Raman spectrum measurement. Residual stress in the conventionally ground PCD was compressive stress; its value was larger than the residual stress in the EDG'ed tools. Residual stress in the EDG'ed PCD tool was tensile stress and its value was smaller.

Residual stress is one of the factors that accelerated the flank wear of PCD tools. The stress at cobalt/diamond interface made the structure unstable and reduced the wear resistance of PCD tools. PCD inserts with bigger residual stress have larger worn area on the flank face after machining. Nano-sized diamond particles found in conventionally ground PCD tools weakened the strength of diamond structure. While, in the EDG'ed PCD tools, this structure did not exist because of the thermal effects of EDG. However, graphitization in EDG'ed PCD tools was more obvious because of the high temperature of plasma which led to large scale of conversion of carbon phases. The presence of graphite affected the stability of diamond structure. EDG'ed PCD tool with less graphitization showed less worn in the machining of titanium alloy.

References

1. Liang L, Liu X, Li X, Li Y (2015) Wear mechanisms of WC–10Ni3Al carbide tool in dry turning of Ti6Al4V. Int J Refract Met Hard Mater 48:272–85
2. Oosthuizen GA, Akdogan G, Dimitrov D, Treurnicht NF (2010) A review of the machinability of titanium alloys. R & D J S Afr Inst Mech Eng 26:43–52
3. Blank V, Popov M, Pivovarov G, Lvova N, Gogolinsky K, Reshetov V (1998) Ultrahard and superhard phases of fullerite C60: comparison with diamond on hardness and wear. Diam Relat Mater 7(2–5):427–31
4. Oosthuizen GA, Akdogan G, Treurnicht N (2011) The performance of PCD tools in high-speed milling of Ti6Al4V. Int J Adv Manuf Technol 52(9-12):929–35
5. Tso PL, Liu YG (2002) Study on PCD machining. Int J Mach Tools Manuf 42(3):331–4
6. Kozak J, Rajurkar K, Wang S (1994) Material removal in WEDM of PCD blanks. J Manuf Sci Eng 116(3):363–9
7. Paggett JW, Drake EF, Griffin ADND (2002) Residual stress and stress gradients in polycrystalline diamond compacts. Int J Refract Met Hard Mater 20(3):187–94
8. Yadav V, Jain VK, Dixit PM (2002) Thermal stresses due to electrical discharge machining. Int J Mach Tools Manuf 42(8):877–88
9. Yahiaoui M, Gerbaud L, Paris J-Y, Denape J, Dourfaye A (2013) A study on PDC drill bits quality. Wear 298–299:32–41
10. Chen F, Gen X, Chunde M, Guoping X (2010) Thermal residual stress of polycrystalline diamond compacts. Trans Nonferrous Metals Soc China 20(2):227–32
11. Jia H, Xiaopeng J, Yue X, Lianru W, Kaikai J, Hongan M (2011) Effects of initial crystal size of diamond powder on surface residual stress and morphology in polycrystalline diamond (PCD) layer. Sci China Phys Mech Astron 54(1):98–101
12. Kalyanasundaram D, Schmidt A, Molian P, Shrotriya P (2014) Hybrid CO2 laser/waterjet machining of polycrystalline diamond substrate: material separation through transformation induced controlled fracture. J Manuf Sci Eng 136(4):041001
13. Weidner DJ, Wang Y, Vaughan MT (1994) Strength of diamond. Science 266(5184):419–22
14. Cheng, K. (2008) Machining dynamics: fundamentals, applications and practices. Springer Science & Business Media.
15. Pan W, Ding S, Mo J (2014) Thermal characteristics in milling Ti6Al4V with polycrystalline diamond tools. Int J Adv Manuf Technol 75(5-8):1077–87
16. Pan W, Kamaruddin A, Songlin D, Mo J (2014) Experimental investigation of end milling of titanium alloys with polycrystalline diamond tools. Proc Inst Mech Eng B J Eng Manuf 228(8):832–44
17. Arsecularatne JA, Zhang LC, Montross C (2006) Wear and tool life of tungsten carbide, PCBN and PCD cutting tools. Int J Mach Tools Manuf 46(5):482–91
18. da Silva RB, Machado AR, Ezugwu EO, Bonney J, Wisley F (2013) Sales, tool life and wear mechanisms in high speed machining of Ti–6Al–4V alloy with PCD tools under various coolant pressures. J Mater Process Technol 213(8):1459–64
19. Li R, Shih AJ (2006) Finite element modeling of 3D turning of titanium. Int J Adv Manuf Technol 29(3-4):253–61
20. Hartung PD, Kramer B, Von Turkovich B (1982) Tool wear in titanium machining. CIRP Ann Manuf Technol 31(1):75–80
21. Kramer B (1987) On tool materials for high speed machining. J Manuf Sci Eng 109(2):87–91
22. Cheng K, Luo X, Ward R, Holt R (2003) Modeling and simulation of the tool wear in nanometric cutting. Wear 255(7–12):1427–32
23. Amin AN, Ismail AF, Khairusshima MN (2007) Effectiveness of uncoated WC–Co and PCD inserts in end milling of titanium alloy—Ti–6Al–4V. J Mater Process Technol 192:147–58

24. Honghua S, Liu P, Fu Y, Xu J (2012) Tool life and surface integrity in high-speed milling of titanium alloy TA15 with PCD/PCBN tools. Chin J Aeronaut 25(5):784–90
25. Li A, Zhao J, Wang D, Zhao J, Dong Y (2013) Failure mechanisms of a PCD tool in high-speed face milling of Ti–6Al–4V alloy. Int J Adv Manuf Technol 67(9-12):1959–66
26. Bhaumik SK, Divakar C, Singh AK (1995) Machining Ti6Al4V alloy with a wBN-cBN composite tool. Mater Des 16(4):221–6
27. Bordin A et al (2015) Analysis of tool wear in cryogenic machining of additive manufactured Ti6Al4V alloy. Wear 328:89–99
28. Cai M, Li X, Rahman M (2007) Study of the mechanism of groove wear of the diamond tool in nanoscale ductile mode cutting of monocrystalline silicon. J Manuf Sci Eng 129(2):281–6
29. Jawaid A, Che-Haron C, Abdullah A (1999) Tool wear characteristics in turning of titanium alloy Ti-6246. J Mater Process Technol 92:329–34
30. Sreejith P, Krishnamurthy R, Malhotra SK, Narayansamy K (2000) Evaluation of PCD tool performance during machining of carbon/phenolic ablative composites. J Mater Process Technol 104(1):53–8
31. Pramanik A, Zhang L, Arsecularatne J (2008) Machining of metal matrix composites: effect of ceramic particles on residual stress, surface roughness and chip formation. Int J Mach Tools Manuf 48(15):1613–25
32. Minton T, Ghani S, Sammler F, Bateman R, Furstmann P, Roeder M (2013) Temperature of internally-cooled diamond-coated tools for dry-cutting titanium. Int J Mach Tools Manuf 75:27–35
33. Rahim M.Z., Songlin D Mo J (2015) Electrical discharge grinding of polycrystalline diamond—effect of machining parameters and finishing in-feed. J Manuf Sci Eng 137:021017–1
34. Bai Q et al (2004) Study on wear mechanisms and grain effects of PCD tool in machining laminated flooring. Int J Refract Met Hard Mater 22(2):111–5
35. Yingfei G, Jiuhua X, Hui Y (2010) Diamond tools wear and their applicability when ultra-precision turning of SiC p/2009Al matrix composite. Wear 269(11):699–708